Hindawi
International Journal of Antennas and Propagation
Volume 2023, Article ID 1832806, 11 pages
https://doi.org/10.1155/2023/1832806

Research Article

Satisfaction-Based Multiobjective Optimization of the Design of a 65 GHz Millimeter-Wave Connector

Xiang Li,[1,2] **Lijun Tong**,[1,2] **Zheng Kong**,[1,2] **Wenju Lu**,[1,2] **and Qian Xie**[1,2]

[1]*Aerospace Internet of Things Technology Co. LTD., Beijing 100094, China*
[2]*China Academy of Aerospace Electronics Technology, Beijing 100094, China*

Correspondence should be addressed to Zheng Kong; kzhengbj@outlook.com

Received 18 August 2022; Revised 19 March 2023; Accepted 3 April 2023; Published 18 April 2023

Academic Editor: Anna Pietrenko-Dabrowska

It is difficult to simultaneously ensure the radio frequency (RF) performance and mechanical strength of 65 GHz millimeter-wave connectors. To address this, satisfaction-based multiobjective method for connector design optimization is proposed. An optimization model is developed for the structural dimensions of 65 GHz millimeter-wave connectors to minimize the voltage standing wave ratio, insertion loss, and deflection and maximum stress of the center conductor. The proposed optimization model concurrently satisfies the design requirements in terms of characteristic impedance, transmission frequency, and dielectric withstanding voltage. The model is optimized by innovatively using the multiobjective chaotic optimization algorithm in microwave finite-element simulations. The resulting optimal structure satisfies all performance requirements, thereby proving the rationality and feasibility of the proposed method. Moreover, this study establishes a novel design for other microwave devices to solve the problem of multiple performance index restrictions.

1. Introduction

The rapid improvement of microwave communications technologies has continuously increased in signal frequency [1–4]. However, 2.92 mm coaxial millimeter-wave connectors cannot support signal frequencies greater than 46 GHz, necessitating the use of millimeter-wave connectors that can support frequencies of 65 GHz and above. However, the complexity of connector design increases exponentially with an increase in the signal transmission frequency because the transmission performance and mechanical strength of a radiofrequency (RF) connector are mutually contradictory at frequencies of 65 GHz and above. As a result, it is extremely difficult to simultaneously satisfy both of these design requirements.

Previous researches on the design of millimeter-wave connectors mainly focused on the influences of a certain structure or size on some microwave parameters [5–7]. Only a few researches were carried out on the optimal design method of connectors. In existing optimal design of RF connector, mathematical methods are used to search for the optimal solution for a given design objective. However, existing methods are not suitable for solving problems with multiple contradicting design objectives. Moreover, their solutions may fail to satisfy even the most fundamental requirements of each objective [8–14]. Therefore, the existing optimal design approach is unsuitable for the design of 65 GHz RF connectors. Consequently, in this study, the multiobjective constraint satisfaction optimization (CSO) approach was utilized to address this design problem.

CSO is an intrinsically multiobjective approach to perform optimization. In contrast to the conventional approach, its aim is to "satisfy" rather than "optimize." The constraints (i.e., performance requirements) and objectives (to-be-optimized parameters) are combined into a homogenous whole that enables increased flexibility and a wider scope of applicability [15–20].

In this study, chaotic optimization was innovatively combined with microwave finite-element simulations to obtain a CSO-based multiobjective chaotic optimization method that could effectively overcome the design problems of 65 GHz·millimeter-wave RF connectors.

2. Design Requirements

The design requirements of the proposed 65 GHz RF connector are listed in Table 1.

The RF performance and mechanical strength are the two most critical performance metrics for RF connectors. Generally, the RF performance is characterized by the voltage standing wave ratio (VSWR) and insertion loss (IL) of the connector. In contrast, the mechanical strength is characterized by metrics that reflect the resistance of the inner and outer conductors to deformation and failure. In the absence of design constraints for the outer conductor, mechanical strength is defined by the resistance of the inner conductor resistance to stress-induced deformation and failure. Therefore, the optimization parameters (objectives) include VSWR, IL, and the deflection and maximum stress of the center conductor. The hard constraints include characteristic impedance, frequency range, and dielectric withstanding voltage (DWV).

3. Optimization Model

3.1. Structure of the Connector. A millimeter-wave connector comprises three parts: an inner conductor, outer conductor, and insulated supports, with a cavity between the inner and outer conductors. There are slots on the inner and outer conductors, which are used to affix insulated supports, as depicted in Figure 1.

The parameters that have the greatest effect on RF performance and mechanical strength are the inner diameter of the outer conductor D_0, the outer diameter of the insulated support D_1, inner diameter of the insulated support d_1, thickness B, and the spacing between each pair of insulated supports A. Since D_0 and d_0 are standardized for this series of connectors, the optimization of connector design primarily concerns the four structural parameters that pertain to the insulated supports: D_1, d_1, B, and A.

3.2. Hard Constraints. According to the design standard for 65 GHz millimeter-wave connectors, three hard constraints exist: characteristic impedance, frequency range, and DWV [21]. Here, the structural parameters of the RF connector are correlated with these constraints based on the connector design theory to obtain the following constraint equations for the optimization process.

3.2.1. Characteristics Impedance. This constraint was constructed based on microwave transmission theory and the standard characteristic impedance for RF connectors.

$$Z_0 = \frac{60}{\sqrt{\varepsilon_r}} \ln \frac{D_1}{d_1} = 50\Omega. \tag{1}$$

In (1), D_1, d_1, and ε_r denote the outer and inner diameters of the insulated supports and the relative permittivity of the insulator material, respectively.

Table 1: Design requirements of the 65 GHz RF connector.

Parameter	Index requirements
Frequency ranges	DC~65 GHz
Characteristic impedance	50 Ω
Voltage standing wave ratio (VSWR)	≤1.40 (The measured values) ≤1.20 (The simulated value)
Insertion loss (IL)	≤0.6 dB (The measured values) ≤0.3 dB (The simulation value)
Dielectric withstanding voltage	≥AC 750 V
Compliance of the central conductor	≤0.076 mm (@20 N)
Shock tolerance	1000 g

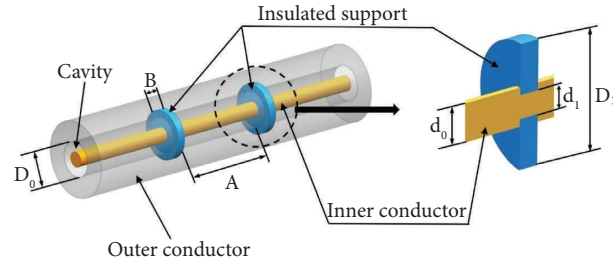

Figure 1: Simplified structure of a millimeter-wave connector.

3.2.2. Transmission Frequency. A uniform coaxial cable transmits electromagnetic waves in the transverse electromagnetic (TEM) mode. However, at the coaxial connector, higher-order modes can be excited if the frequency of the transmitted electromagnetic wave exceeds a certain threshold. In TEM single-mode operation, the TE_{11} mode has the lowest cut-off frequency among all higher-order modes. Since its cut-off frequency f_c should be greater than the maximum frequency stipulated by the design requirements, the following constraint is constructed:

$$f_c = \frac{2C_0}{\pi(D_1 + d_1)\sqrt{\varepsilon_r}} \geq 65\text{GHz}, \tag{2}$$

where C_0 indicates the speed of light in vacuum.

According to the coaxial transmission line theory, the occurrence of higher-order modes in a coaxial cable depends on the thickness and spacing of the insulated supports. To prevent the occurrence of the H_{10} (TE_{10}) higher-order mode, the thickness B and spacing A of the insulated supports must satisfy the following conditions:

$$B < \frac{\lambda_g}{\pi} \tan^{-1}\left[\frac{\sqrt{(f_c/f)^2 - 1}}{\sqrt{\varepsilon_r}\sqrt{1 - 1/\varepsilon_r (f_c/f)^2}}\right], \tag{3}$$

$$A \geq 2D_0, \tag{4}$$

where λ_g denotes the working wavelength of the coaxial line, f indicates the working frequency, and f_c signifies the cut-off frequency.

3.2.3. Dielectric Withstanding Voltage (DWV). The DWV of a RF connector denotes the maximum voltage that can be loaded on the insulator between the inner and outer conductors without current flowing through the insulator. The following constraint is constructed based on the design requirement for RF connectors:

$$U_a = \frac{d_1}{2\sqrt{\varepsilon_r}} \ln \frac{D_1}{d_1} \bullet E_{\max} \geq 750\text{V}, \tag{5}$$

where $E_{\max}$ denotes the DWV of the insulator.

3.3. Optimization Objectives. The optimization objectives are parameters that pertain to the mechanical strength and RF performance of the connector. The parameters that reflect the mechanical strength of an RF connector are $\sigma_{\max}$ (the maximum stress inside the center conductor caused by shock G) and the deflection s that occurs in the insulator when the center conductor is subjected to an axial force. The smaller the values, the better the mechanical strength of the RF connector. The parameters that reflect RF performance are VSWR and IL; the smaller the values, the better the RF performance of the connector. Therefore, the optimization objectives are $\sigma_{\max}$ and s, and the maximum VSWR ($\text{VSWR}_{\max}$) and IL ($\text{IL}_{\max}$) values of the RF connector are in the DC-65 GHz range.

Based on the structure of millimeter-wave RF connectors, the aforementioned optimization objectives were correlated with the structural dimensions of the connector. First, we determine the relationship between the structural dimensions of the connector and its mechanical strength by modeling the structure of the connector as a simply supported beam. According to this model, a shock G will generate a maximum moment of $M_{\max} = \pi d_0^2 \rho G A^2/32$.

The maximum flexural stress of the center conductor [22] is then given by

$$\sigma_{\max} = \frac{32M_{\max}}{\pi d_0^3} = \frac{\rho G A^2}{d_0}, \tag{6}$$

where ρ denotes the density of center conductor.

The axial deflection of the insulator [22] is approximated by

$$s \approx \frac{3F\left(1-\mu^2\right)R^2}{8\pi E B^3}, \tag{7}$$

where F denotes the axial force applied on the center conductor and transferring to the insulator, μ indicates Poisson's ratio of insulator, R signifies the radius of insulator, E denotes elastic modulus of insulator, and B indicates the thickness of insulator.

As shown above, the strength of the connector increases with increasing insulator thickness (B) and decreasing insulator spacing (A). However, according to the microwave transmission theory, RF performance improves with decreasing B and increasing A. This contradiction complicates the design of 65 GHz·millimeter-wave connectors. Furthermore, considering the absence of a direct relationship between the structural dimensions of the connector and its VSWR and IL, microwave simulations must be employed to solve for these parameters. This requirement complicates the design optimization of millimeter-wave connectors. Therefore, a multiobjective chaotic optimization algorithm was used to solve these problems.

3.4. Multiobjective Chaotic Optimization Algorithm. It is difficult to find optimal solutions in multiobjective optimization problems. Instead, the more practical approach is to search for a sufficiently optimal solution that balances all of the objectives, according to the requirements of the given application, which is called a "satisfactory solution" [23]. To obtain the satisfactory solution for the current problem, the objective functions and constraints of the optimization problem were fuzzified. Subsequently, a search was conducted for the satisfactory solution that optimizes the optimization objectives while satisfying all design constraints in the fuzzy set containing the solutions that optimize each objective.

The chaotic optimization method uses the ergodicity of chaos to ensure that the algorithm does not get stuck in local minima when searching for a solution [24, 25]. The fundamental principles of chaotic optimization are as follows: first, the ergodic paths generated by a deterministic iteration are used to examine the solution space. When a predetermined termination condition is satisfied, the search is deemed to have discovered an optimal state that approaches the optimal solution to the problem. This point is then used as the starting point of the "fine search" in the subsequent step [26]. In this study, the chaotic optimization algorithm was utilized to optimize the structural dimensions of the 65 GHz·millimeter-wave connector: the fundamental structural parameters of the connector were orthogonally transformed in large steps within the feasible solution space until a solution with a high overall satisfaction for all objective parameters was found. Subsequently, a fine search was performed in the vicinity of this solution until the solution that optimizes satisfaction in all objective parameters is found.

Based on the characteristics of the objective functions, the satisfaction function is developed to minimize the objective functions while satisfying all hard constraints. The satisfaction function has a lower bound without an upper bound, and the lower bound is the optimal value that corresponds to all of the objectives reaching their optimal values. Therefore, the satisfaction function was developed to be a two-stage linear function that is flat in the first stage and descending in the second stage (Figure 2). This function is described as follows:

$$\mu\left(f_k(X)\right) = \begin{cases} 1, & f_k(X) < c_{0k}, \\ \dfrac{c_{0k} + \delta_{0k} - f_k(X)}{\delta_{0k}}, & c_{0k} \leq f_k(X) \leq c_{0k} + \delta_{0k}, \\ 0, & f_k(X) \geq c_{0k} + \delta_{0k}, \end{cases} \tag{8}$$

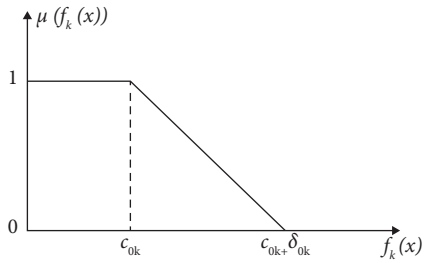

Figure 2: Satisfaction function.

where X represents the vector of the decision variable, where $X = (x_1, x_2, \ldots, x_n)$, i.e., the set of all objective parameters, $f_k(X)$ represents the k-th objective function, where $k = 1, 2, \ldots, p$, with p being the number of objective functions, $\mu(f_k(X))$ represents the satisfaction function of objective $f_k(X)$, c_{ok} denotes the optimal value of $f_k(X)$ in single-objective optimization, and δ_{ok} indicates the increment to objective $f_k(X)$ that is acceptable for the decision maker.

The algorithm that was used to solve the multiobjective connector design problem is described as follows:

Step 1: The following algorithm is used to solve for the constrained optimal solution for each objective function:

$$\begin{cases} \min f_i(X), & i = 1, 2, \cdots, p, \\ s.t. & g_i(X) \le 0, i = 1, 2, \cdots, m, \\ h_j(X) = 0, & j = 1, 2, \cdots l, \end{cases} \tag{9}$$

where $g_i()$ represents the constraint of the i-th inequality, i indicates the numbering of each inequality constraint, m denotes the number of inequality constraints, $h_j(X)$ indicates the constraint of the j-th equality, j denotes the numbering of each equality constraint, and l corresponds to the number of equality constraints.

Step 2: The value of each objective is increased/decreased to determine the value of δ_{ok}.

Step 3: Each single-objective function is fuzzified to determine their satisfaction functions. The satisfaction for all of the objective functions is then redefined as follows:

$$\lambda = \min\left\{\mu(f_1(X)), \mu(f_2(X)), \cdots \mu\left(f_p(X)\right)\right\}. \tag{10}$$

Step 4: c_{ok} and δ_{ok} are substituted into (8) to obtain the expressions of p satisfaction functions.

Step 5: Based on the max-min rule of fuzzy set theory, the multiobjective problem is converted into a single-objective fuzzy nonlinear problem to maximize satisfaction. The mathematical model is described as follows:

$$\begin{cases} \max \lambda, \\ f_k(X) + \lambda\delta_{0k} \le c_{0k} + \delta_{0k}, k = 1, 2, \cdots p, \\ 0 \le \lambda \le 1, \\ g_i(X) \le 0, i = 1, 2, \cdots, m, \\ h_j(X) = 0, j = 1, 2, \cdots l. \end{cases} \tag{11}$$

Step 6: The optimization model is solved using the multiobjective chaotic optimization algorithm, which searches for the optimal solution that gives >90% satisfaction in all objective functions.

4. Optimal Configuration and Results

The design of a 65 GHz millimeter-wave connector is optimized using multiobjective chaotic optimization, according to its design requirements. The parameters of the satisfaction function of each optimization objective are defined as follows:

$$\begin{cases} \text{maximum stress in the center conductor,} \\ \sigma_{\max} = f_1(X), c_{01} = \dfrac{[\sigma]}{10}, c_{01} + \delta_{01} = \dfrac{[\sigma]}{3}, \\ \text{deflection of the center conductor,} \\ s = f_2(X), c_{02} = 0.015\text{mm}, c_{02} + \delta_{02} = 0.076\text{mm}, \text{F} = 20\text{N}), \\ \text{maximum VSWR,} \\ \text{VSWR}_{\max} = f_3(X), c_{03} = 1.01, c_{03} + \delta_{03} = 1.20, \\ \text{maximum } IL, \\ IL_{\max} = f_4(X), c_{04} = 0.08\text{dB}, c_{04} + \delta_{04} = 0.30\text{dB}, \end{cases} \tag{12}$$

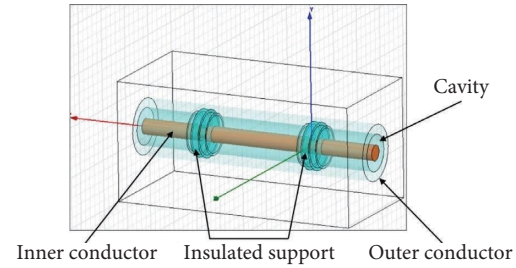

Figure 3: Basic model of the 65 GHz·millimeter-wave connector.

where $[\sigma]$ denotes the permissible stress of the material of the center conductor. $\sigma_{\max}$ and s are calculated using (6) and (7), respectively. Since $\mathrm{VSWR}_{\max}$ and $\mathrm{IL}_{\max}$ depend on the combined actions of various factors, they cannot be calculated by an empirical function, so they must be computed using finite simulation software. This is one aspect where the RF connector design differs from ordinary multiobjective optimization problems.

The method described in Section 3.4 is combined with the finite-element simulation to optimize the structural dimensions of the millimeter-wave connector, as described as follows:

(a) According to equation (1), the outer and inner diameters of the insulated support (D_1 and d_1) are correlated variables. Hence, the structure of the insulated supports is defined by three independent variables, outer diameter D_1, thickness B, and spacing A. The parameter optimization is performed using these three independent variables.

(b) According to the equations (2)–(5) along with the structural characteristics and mechanical constraints of the connector, the ranges of the three independent variables are $D_1{}' \le D_1 \le D_1{}''$, $\mathrm{B}' \le B \le B''$, and $\mathrm{A}' \le A \le A''$. Let the initial values of these variables be $D_{10} = D_1{}'$, $B_0 = \mathrm{B}'$, and $A_0 = A'$. The values of ε_r and $E_{\max}$ of PEI (Polyetherimide) material for insulator in this study are 3.15 and 27 kV/mm, respectively. Subsequently, a model of the 65 GHz RF connector is constructed in the Ansys high-frequency structure simulator (HFSS) (Figure 3), which is used to perform the microwave simulations (Figure 4) required to calculate $\mathrm{VSWR}_{\max}$ and $\mathrm{IL}_{\max}$ of the connector. The bulk conductivity of copper for conductor is 5.8×10^7 s/m in the FEM simulation.

(c) The parameters are incremented by one step, within the aforementioned range: $D_1{}' \le \mathrm{D}_{1r} = D10 + r\Delta_{D1} \le D1''$, $B' \le B_t = B0 + t\Delta B \le B''$, $A' \le A_q = A_0 + q\Delta_A \le A''$. Another simulation is performed to compute the microwave parameters of the new structure (Figure 5) that yields its $\mathrm{VSWR}_{\max}$ and $\mathrm{IL}_{\max}$ values. Equations (6) and (7) are used to calculate $\sigma_{\max}$ and s, and the resulting objective parameters are substituted into (8), (10), and (12) to compute the overall satisfaction of the design, as listed in Table 2. Once all of the stepwise changes in the fundamental parameters have been performed and their corresponding overall satisfaction values have been calculated, the best solution from this round of computations is selected.

(d) Following the first round of computations, a solution that yields a high overall satisfaction for the objective parameters was found. The solution was then used as the initial values of the structural parameters for the next round of optimization. This subsequent round is performed with smaller incremental steps to conduct a finer search in the vicinity of the current solution and find a solution that provides a better overall satisfaction value.

(e) The above process is iteratively repeated until the difference between the current and immediately preceding searches is smaller than a predetermined threshold (e.g., 0.005). At the end of the search, it may be concluded that all of the objective parameters have attained their optimal satisfaction values.

The design of the 65 GHz·millimeter-wave connector that was optimized using the aforementioned scheme is presented in Figures 6 and 7, and Table 3.

In Table 3, Figures 6, and 7, it is shown that the optimization reduced $\mathrm{VSWR}_{\max}$ from 1.2234 to 1.0183, which is a significant improvement in RF performance. Furthermore, all the satisfaction values of the mechanical strength and RF performance parameters are greater than 0.9, which indicates that all parameters have been optimized to a highly satisfactory level. According to the optimized parameters, a 65 GHz millimeter-wave connector was manufactured (Figure 8). The measured VSWR and insertion loss results are illustrated in Figure 9 and 10, with a maximum value of 1.13 and 0.32 dB, respectively, which satisfies the design requirements of Table 1 and achieves excellent performance. The tests verify that the compliance of the central conductor, the shock tolerance, and other index requirements satisfy the requirements of Table 1 by a large margin.

Hence, the connector dimensions obtained by multiobjective chaotic optimization provide a satisfactory level of mechanical strength while ensuring excellent RF performance. Thus, we can conclude that the proposed design method can effectively and simultaneously satisfy multiple performance requirements of a product.

Compared with traditional methods, the novelties of this method are listed in Table 4. This method is advantageous in terms of design efficiency and indicators.

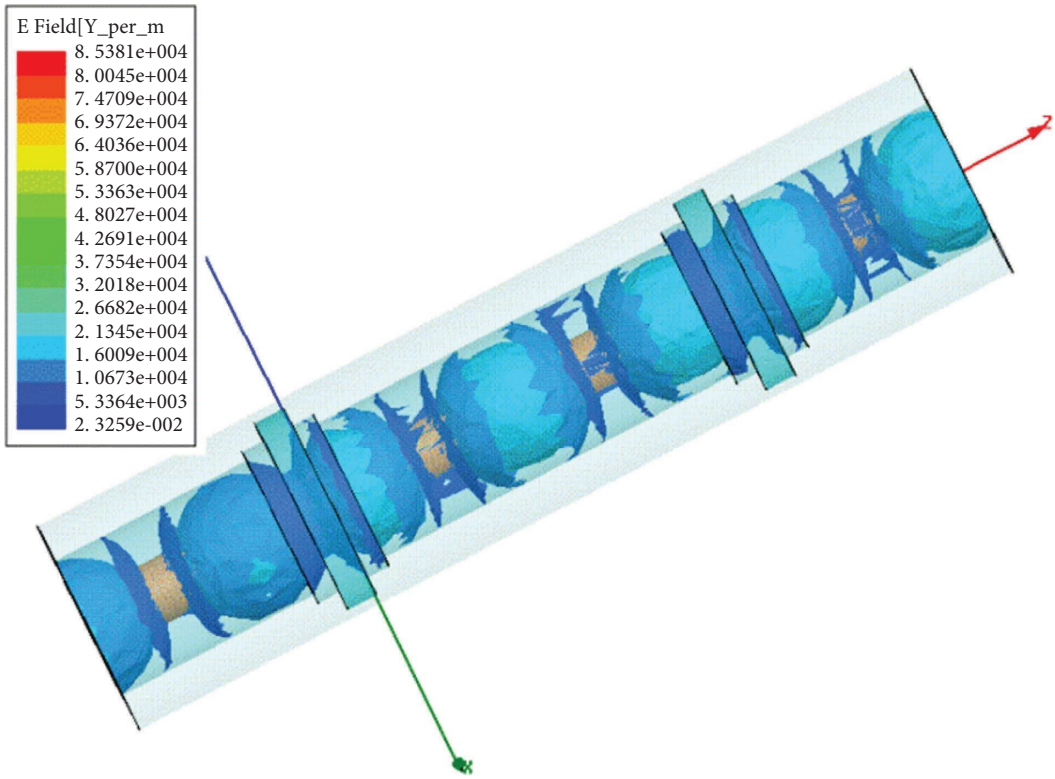

Figure 4: Finite element microwave simulation of the connector.

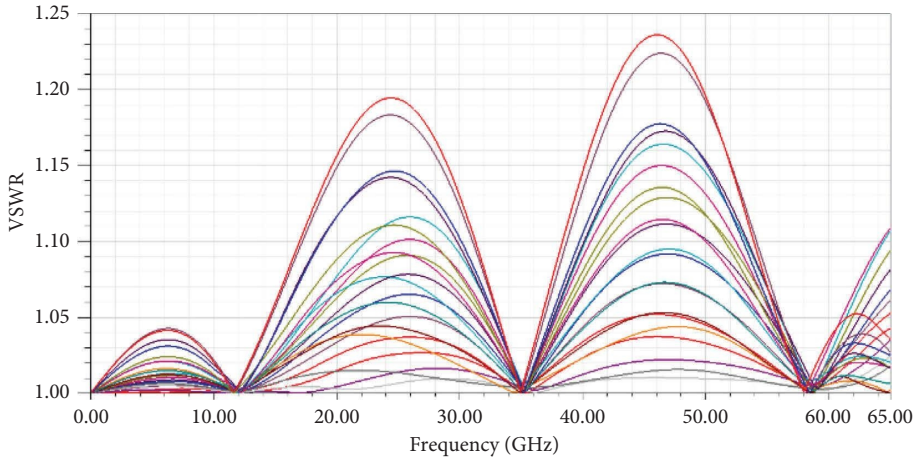

Figure 5: Simulated VSWR values for each set of structural parameters.

Table 2: Satisfaction of each objective parameter after optimization.

Basic parameters	σ_{max}	s	$VSWR_{max}$	IL_{max}	Overall satisfaction λ
D_{10}, B_0, A_0	$f_1(X_{000})$	$f_2(X_{000})$	$f_3(X_{000})$	$f_4(X_{000})$	$\min\{\mu(f_1(X_{000}))\ldots\mu(f_4(X_{000}))\}$
D_{11}, B_0, A_0	$f_1(X_{100})$	$f_2(X_{100})$	$f_3(X_{100})$	$f_4(X_{100})$	$\min\{\mu(f_1(X_{100}))\ldots\mu(f_4(X_{100}))\}$
—	—	—	—	—	—
D_{1r}, B_t, A_q	$f_1(X_{rtq})$	$f_2(X_{rtq})$	$f_3(X_{rtq})$	$f_4(X_{rtq})$	$\min\{\mu(f_1(X_{rqt}))\ldots\mu(f_4(X_{rqt}))\}$
—	—	—	—	—	—

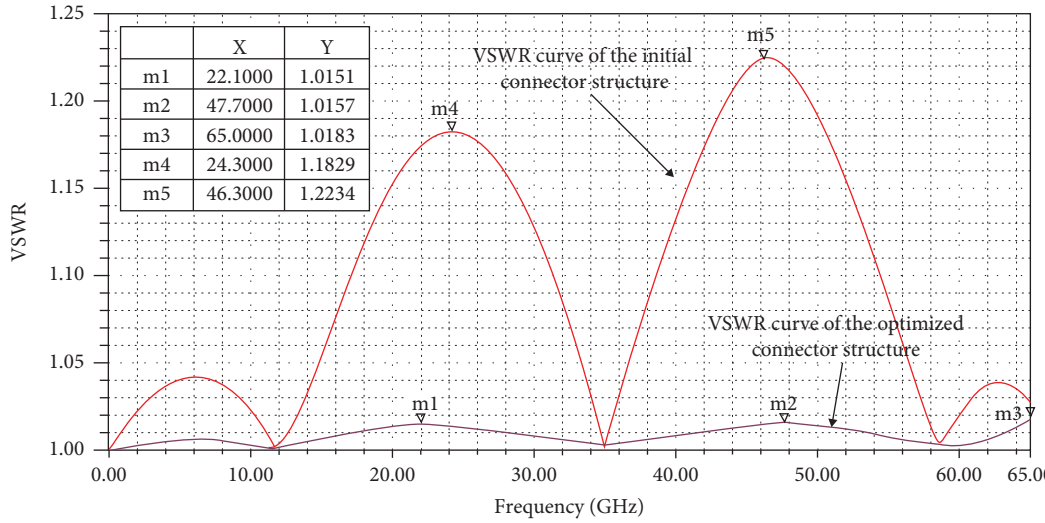

Figure 6: Comparison of the connector's VSWR curves before and after optimization.

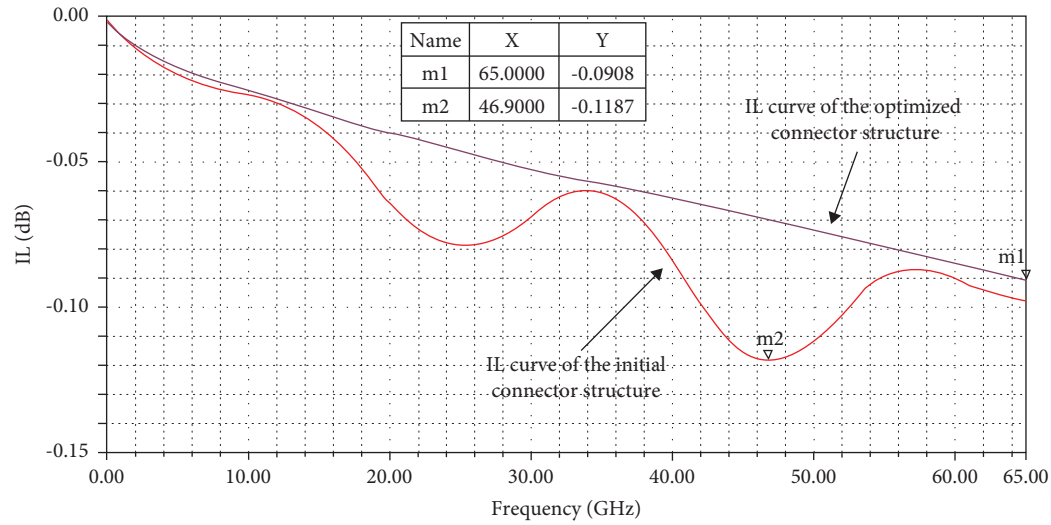

Figure 7: Comparison of the connector's IL curves before and after optimization.

Table 3: Optimized structural parameters and the satisfaction of each objective parameter.

D_1	B			A
2.56 mm	0.38 mm			5.49 mm
σ_{max}	s	VSWR$_{max}$		IL_{max}
3.06 MPa	0.01763 mm	1.0183		0.0908 dB
μ (f_1 (x))	μ (f_2 (x))	μ (f_3 (x))	μ (f_4 (x))	Overall satisfaction λ
1	0.957	0.956	0.951	0.951

Figure 8: 65 GHz·millimeter-wave connector.

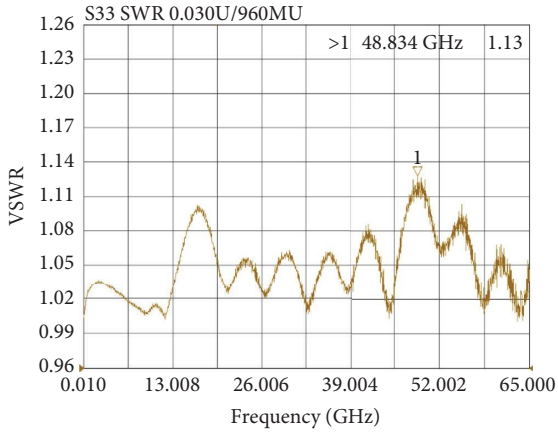

Figure 9: Measured VSWR curve of the connector.

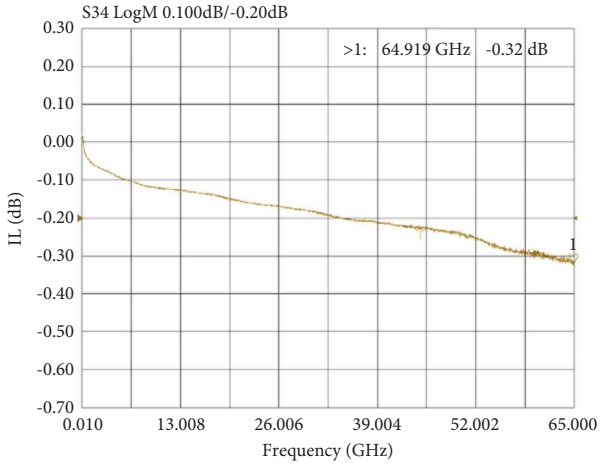

Figure 10: Measured IL curve of the connector.

Table 4: Analysis of novelty and application effect.

Method	Adopted method and novelty	Effect of application
Design of traditional millimeter-wave connector	Microwave simulation and mechanical calculation are separated, and the preferable results obtained from microwave simulation are substituted into other constraint conditions. If they satisfy the requirements, the design stops; else, the parameters are adjusted, and the calculation is reattempted	Repeated attempts are required with low efficiency with a heavy reliance on rich design experiences. It is difficult to obtain satisfactory design results for all indicators
Design of millimeter-wave connector in this study	The satisfaction evaluation method is innovatively adopted to combine microwave simulation and mechanical calculation. Subsequently, the ergodic paths generated iteratively by chaos algorithm is employed to examine the solution space and determine the optimal solution	Repeated attempts are not required. It is designed by determined algorithm with high efficiency and satisfactory results for all indicators

5. Conclusions

(1) In this study, an optimization model for 65 GHz·millimeter-wave connectors was constructed based on the constraint satisfaction optimization (CSO) method, which considers all of the design requirements of these connectors. The model was used to tune the structural dimensions of the connector to ensure that hard constraints, such as the characteristic impedance, transmission frequency, and dielectric withstanding voltage (DWV), were satisfied, while optimizing (minimizing) the voltage standing wave ratio (VSWR), insertion loss (IL), center conductor deflection (s), and the maximum stress of the center conductor (σ_{max}) of the connector.

(2) Multiobjective chaotic optimization was combined with microwave finite-element simulations to optimize the structural parameters of the connector. The optimized connector satisfies all mechanical strength and RF performance requirements, and the satisfaction of each objective parameter is greater than 90%. Thus, the proposed method simultaneously satisfies the contradicting performance requirements in RF connectors. Consequently, it is a powerful tool for designers and clients in this field of study. In summary, this study has effectively established a new approach for the design of millimeter-wave connectors and other microwave devices.

Data Availability

The data used to support the findings of this study are available from the corresponding author on reasonable request.

Conflicts of Interest

The authors declare that there are no conflicts of interest regarding the publication of this paper.

Authors' Contributions

Xiang Li received the B. Eng. degree in Mechanical Engineering and Ph.D. degree in Mechanical Manufacturing from Beijing University of Aeronautics and Astronautics (BUAA), Beijing, China, in 2005 and 2011, respectively. He is currently a researcher of electromechanical device technology with China Academy of Aerospace Electronics Technology. His current research interests include satellite borne microwave device design, electrical contact reliabilities, and passive intermodulation. Lijun Tong received the M.S. degree from Beijing Institute of Technology, Beijing, China, in 2012. She is currently a senior engineer of electronic engineering with China Academy of Aerospace Electronics Technology. Her current research interests include microwave simulation and optimization of radio frequency device. Zheng Kong received the Ph.D. degree in Mechanical Engineering from University of Science and Technology Beijing (USTB), Beijing, China, in 2018. He is currently a senior engineer of electromechanical device technology with China Academy of Aerospace Electronics Technology. His current research interests include design and simulation analysis of electromechanical device. Wenju Lu received the M.S. degree from the Beijing University of Technology, Beijing, China, in 2021. He is currently a engineer of electronic engineering with China Academy of Aerospace Electronics Technology. His current research interests include photoelectric device design and intelligent photoelectric detection. Qian Xie received the M.S. degree in mechanical engineering at Beijing Institute of Technology, Beijing, China, in 2017. She is currently an engineer of electromechanical device technology with China Academy of Aerospace Electronics Technology. Her current research interests include design and development of microwave components.

Acknowledgments

This work was supported in part by the Innovation Research and Development Fund of China Academy of Aerospace Electronics Technology.

References

[1] Q. Li, J. Gao, G. T. Flowers, Z. Cheng, G. Xie, and R. Ji, "Modeling and analysis of radio frequency connector degradation using time domain reflectometry technique," *International Journal of RF and Microwave Computer-Aided Engineering*, vol. 30, Article ID e22271, 2020.

[2] S.-P. Gao, I. Cherukhin, and Y. Guo, "Characterizing microwave connectors over temperature: thermal-stable standards and characterization method," *IEEE Transactions on Microwave Theory and Techniques*, vol. 70, no. 2, pp. 1078–1086, 2022.

[3] H. Yang, W. Huang, H. Wen, and X. Y. Zhang, "Improved design of flange mount coaxial connector with low passive intermodulation distortion," *IEEE Transactions on Instrumentation and Measurement*, vol. 71, Article ID 5501307, pp. 1–7, 2022.

[4] D. Matos, R. Correia, and N. B. Carvalho, "Millimeter-wave hybrid RF-DC converter based on a GaAs chip for IoT-WPT applications," *IEEE Microwave and Wireless Components Letters*, vol. 31, no. 6, pp. 787–790, June 2021.

[5] Y. C. Huang, C. P. Chao, M. J. Gao et al., "A low-profile RF wire-to-board connector design for millimeter wave applications," in *Proceedings of the 2020 IEEE USNC-CNC-URSI North American Radio Science Meeting (Joint with AP-S Symposium)*, pp. 13-14, Toronto, ON, USA, July 2020.

[6] R. B. Hsu, Y. C. Huang, C. C. Lee et al., "High frequency and high speed connector design for 5G applications," in *Proceedings of the 2021 IEEE International Symposium on Radio-Frequency Integration Technology (RFIT)*, pp. 1–3, Busan, South Korea, August 2021.

[7] M. Motoyoshi, W. Ye, S. Kameda, and N. Suematsu, "Side coaxial connector feed design for a millimeter-wave patch antenna measurement," in *Proceedings of the 2016 International Symposium on Antennas and Propagation (ISAP)*, pp. 1046-1047, Okinawa, Japan, October, 2016.

[8] S. Koziel, A. Bekasiewicz, and S. Szczepanski, "Multi-objective design optimization of antennas for reflection, size, and gain

variability using kriging surrogates and generalized domain segmentation," *International Journal of RF and Microwave Computer-Aided Engineering*, vol. 28, no. 5, Article ID e21253, 2018.

[9] A. Bekasiewicz, S. Koziel, and Q. S. Cheng, "Analysis of circular polarization antenna design trade-offs using low-cost EM-driven multiobjective optimization," *International Journal of RF and Microwave Computer-Aided Engineering*, vol. 29, Article ID e21483, 2018.

[10] S. Koziel and A. Bekasiewicz, "Rapid simulation-driven multiobjective design optimization of decomposable compact microwave passives," *IEEE Transactions on Microwave Theory and Techniques*, vol. 64, no. 8, pp. 2454–2461, 2016.

[11] G. Chiandussi, M. Codegone, S. Ferrero, and F. Varesio, "Comparison of multi-objective optimization methodologies for engineering applications," *Computers & Mathematics with Applications*, vol. 63, no. 5, pp. 912–942, 2012.

[12] C. Li, F. You, T. Yao et al., "Simulated annealing particle swarm optimization for high-efficiency power amplifier design," *IEEE Transactions on Microwave Theory and Techniques*, vol. 69, no. 5, pp. 2494–2505, 2021.

[13] M. Soltanifar, "An investigation of the most common multi-objective optimization methods with propositions for improvement," *Decision Analytics Journal*, vol. 1, Article ID 100005, 2021.

[14] H. M. Torun and M. Swaminathan, "High-dimensional global optimization method for high-frequency electronic design," *IEEE Transactions on Microwave Theory and Techniques*, vol. 67, no. 6, pp. 2128–2142, 2019.

[15] S. Petchrompo, D. W. Coit, A. Brintrup, A. Wannakrairot, and A. K. Parlikad, "A review of Pareto pruning methods for multi-objective optimization," *Computers & Industrial Engineering*, vol. 167, Article ID 108022, 2022.

[16] J. Ji and M. Wong, "An improved dynamic multi-objective optimization approach for nonlinear equation systems," *Information Sciences*, vol. 576, pp. 204–227, 2021.

[17] Y. Tian, Y. Zhang, Y. Su, X. Zhang, K. C. Tan, and Y. Jin, "Balancing objective optimization and constraint satisfaction in constrained evolutionary multiobjective optimization," *IEEE Transactions on Cybernetics*, vol. 52, no. 9, pp. 9559–9572, 2022.

[18] H. Jiang, C. K. Kwong, W. H. Ip, and Z. Chen, "Chaos-based fuzzy regression approach to modeling customer satisfaction for product design," *IEEE Transactions on Fuzzy Systems*, vol. 21, no. 5, pp. 926–936, 2013.

[19] X. Zhang, G. Tan, Z. Liu, Q. Wang, W. Zhang, and T. Xia, "Finite control set model predictive direct power control of single-phase three-level PWM rectifier based on satisfactory optimization," *IEEE Access*, vol. 9, pp. 11479–11491, 2021.

[20] M. T. Touati, S. Li, J. Wu, M. Ali, and M. M. Khan, "Satisfactory model predictive control for a hybrid single-phase seven-level converter," *CSEE Journal of Power and Energy Systems*, vol. 7, no. 5, pp. 1102–1112, 2021.

[21] Z. Wu et al., "Design theory basis and formula," in *Rf Connector Design and Paper Compilation*, pp. 10–76, S.X. press, Xi'an, China, 2005.

[22] F. P. Beer, E. R. Johnston, J. T. Dewolf, and D. F. Mazurek, *Statics and Mechanics of Materials*, China Machine Press, Baiwanzhuang, China, 2014.

[23] L. Zheng, *Multi-objective Hybrid Chaos Optimization Algorithm and its Application*Journal of Ningxia University, Yinchuan, China, 2012.

[24] H. Wang, Y. Kang, and B. Li, "Synthesis for sidelobe suppression of linear array based on improved grasshopper optimization algorithm with adaptive chaotic strategy," *International Journal of RF and Microwave Computer-Aided Engineering*, vol. 32, no. 4, Article ID e23048, 2022.

[25] P. Pan, D. Wang, and B. Niu, "Design optimization of APMEC using chaos multi-objective particle swarm optimization algorithm," *Energy Reports*, vol. 7, no. 6, pp. 531–537, 2021.

[26] L. Wang, D. Zhen, and Q. Li, "Research progress of chaos optimization methods," *Computing Technology and Automation*, vol. 20, no. 1, pp. 1–5, 2001.